

Figure C-1. Map of Study Area.

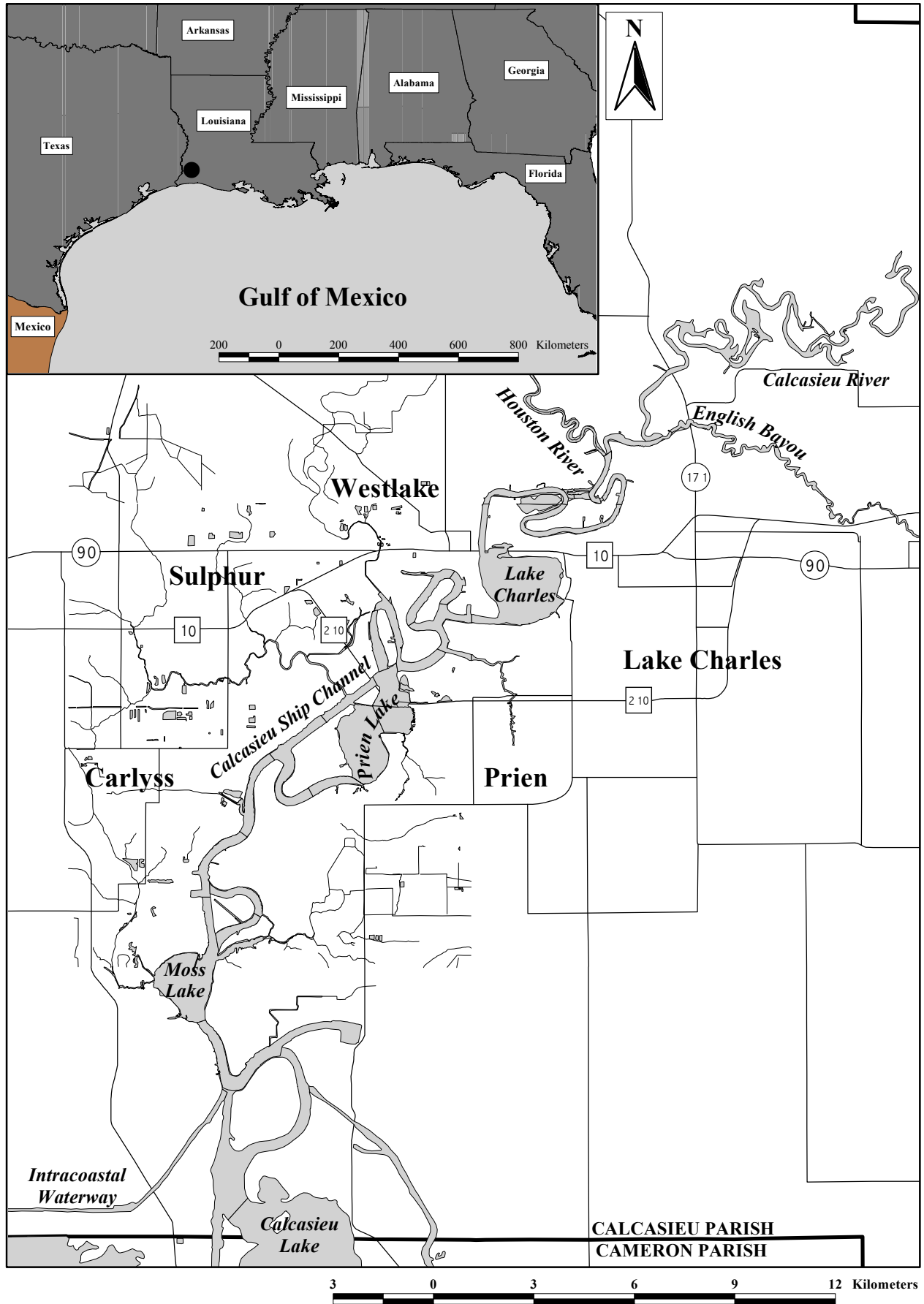


Figure C-2. Map of the Upper Calcasieu River AOC, showing locations of sampling sites for whole-sediment chemistry (WSC) and solid phase tests with the bacterium, *Vibrio fisheri* (VF).

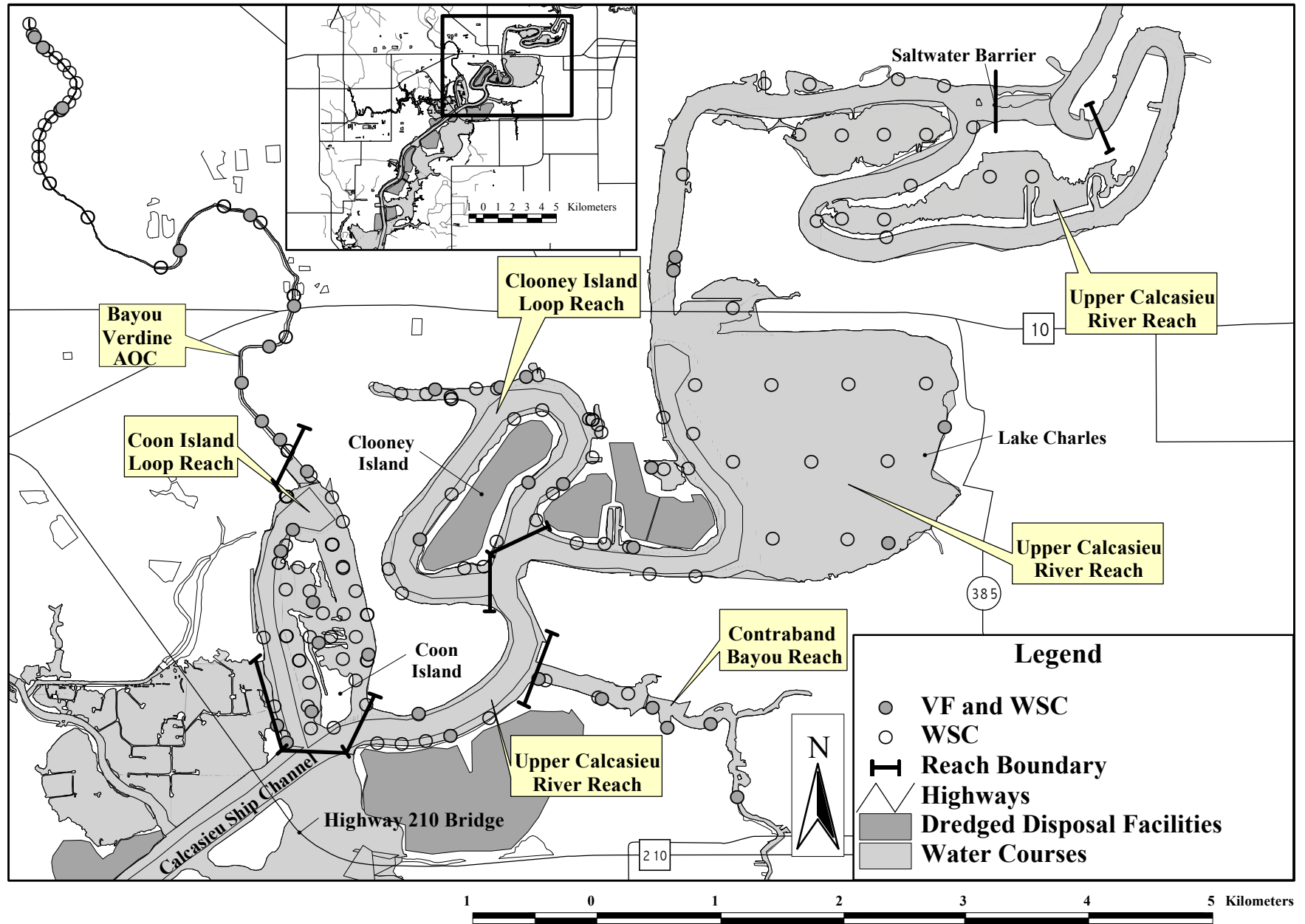


Figure C-3. Map of the Bayou d'Inde AOC, showing locations of sampling sites for whole-sediment chemistry (WSC) and solid phase tests with the bacterium, *Vibrio fisheri* (VF).

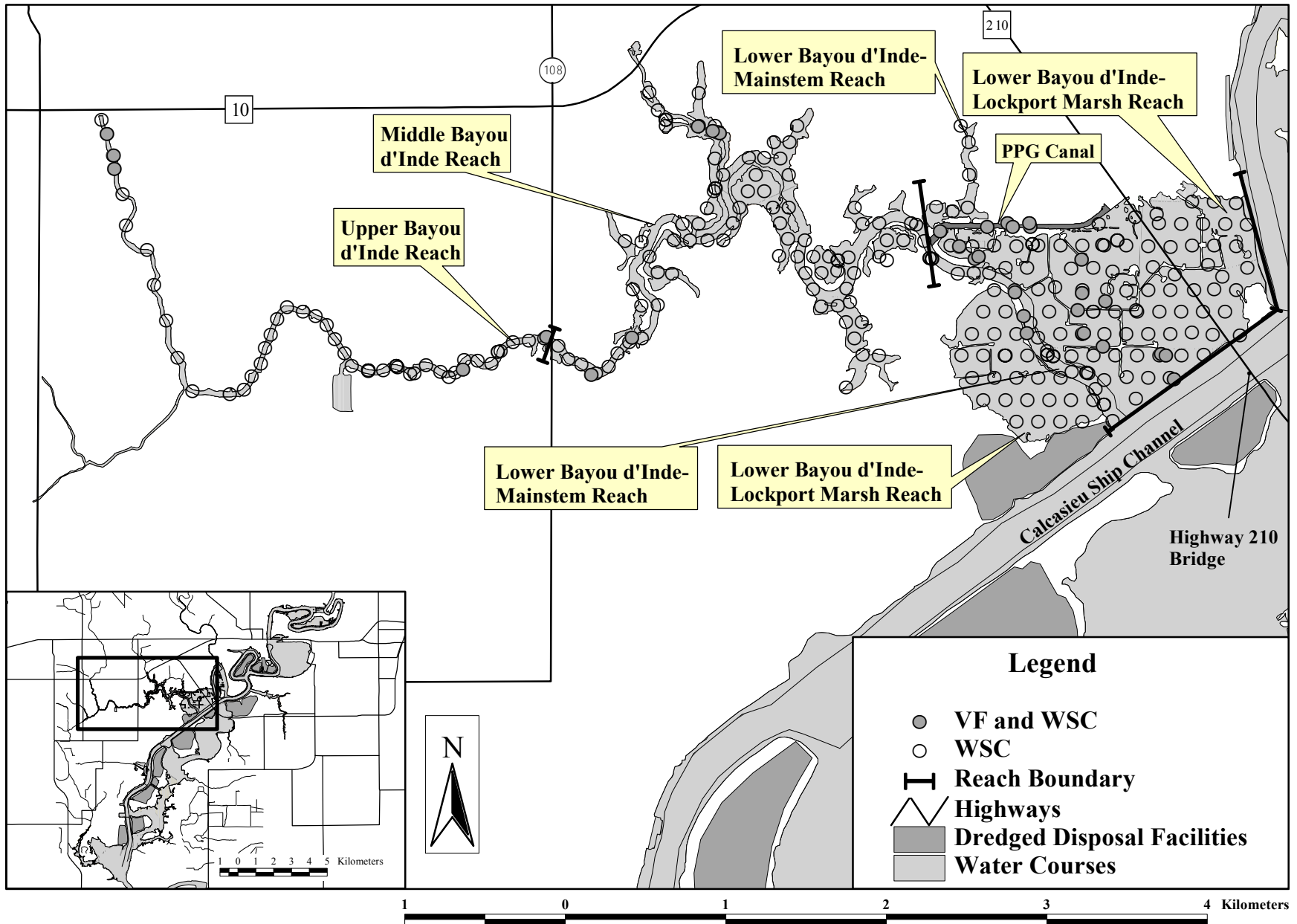


Figure C-4a. Map of the upper Middle Calcasieu River AOC, showing locations of sampling sites for whole-sediment chemistry (WSC) and solid phase tests with the bacterium, *Vibrio fisheri* (VF).

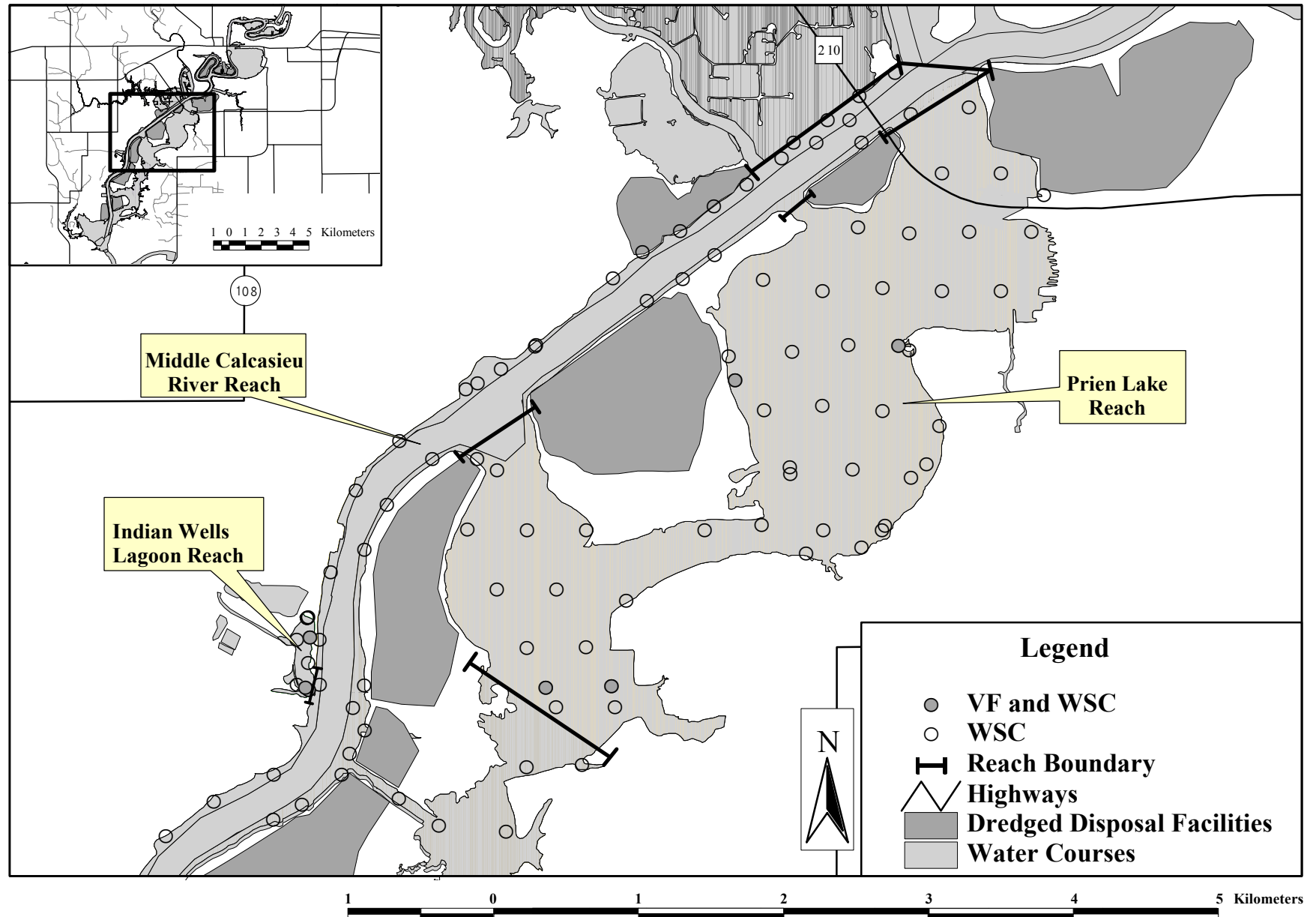


Figure C-4b. Map of the lower Middle Calcasieu River AOC, showing locations of sampling sites for whole-sediment chemistry (WSC) and solid phase tests with the bacterium, *Vibrio fisheri* (VF).

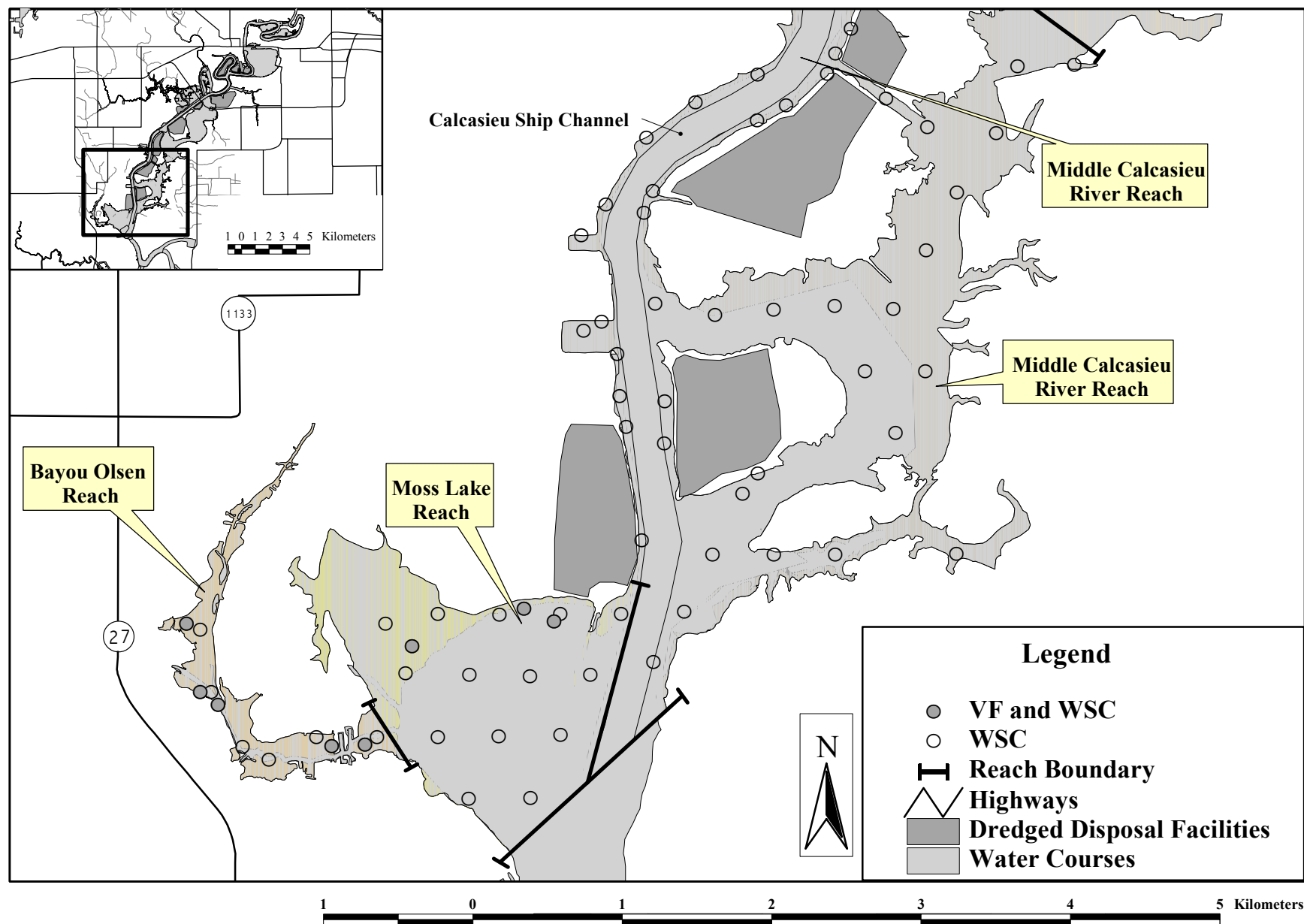


Figure C-5. Map of the Reference Areas, showing locations of sampling sites for whole-sediment chemistry (WSC) and solid phase tests with the bacterium, *Vibrio fisheri* (VF).

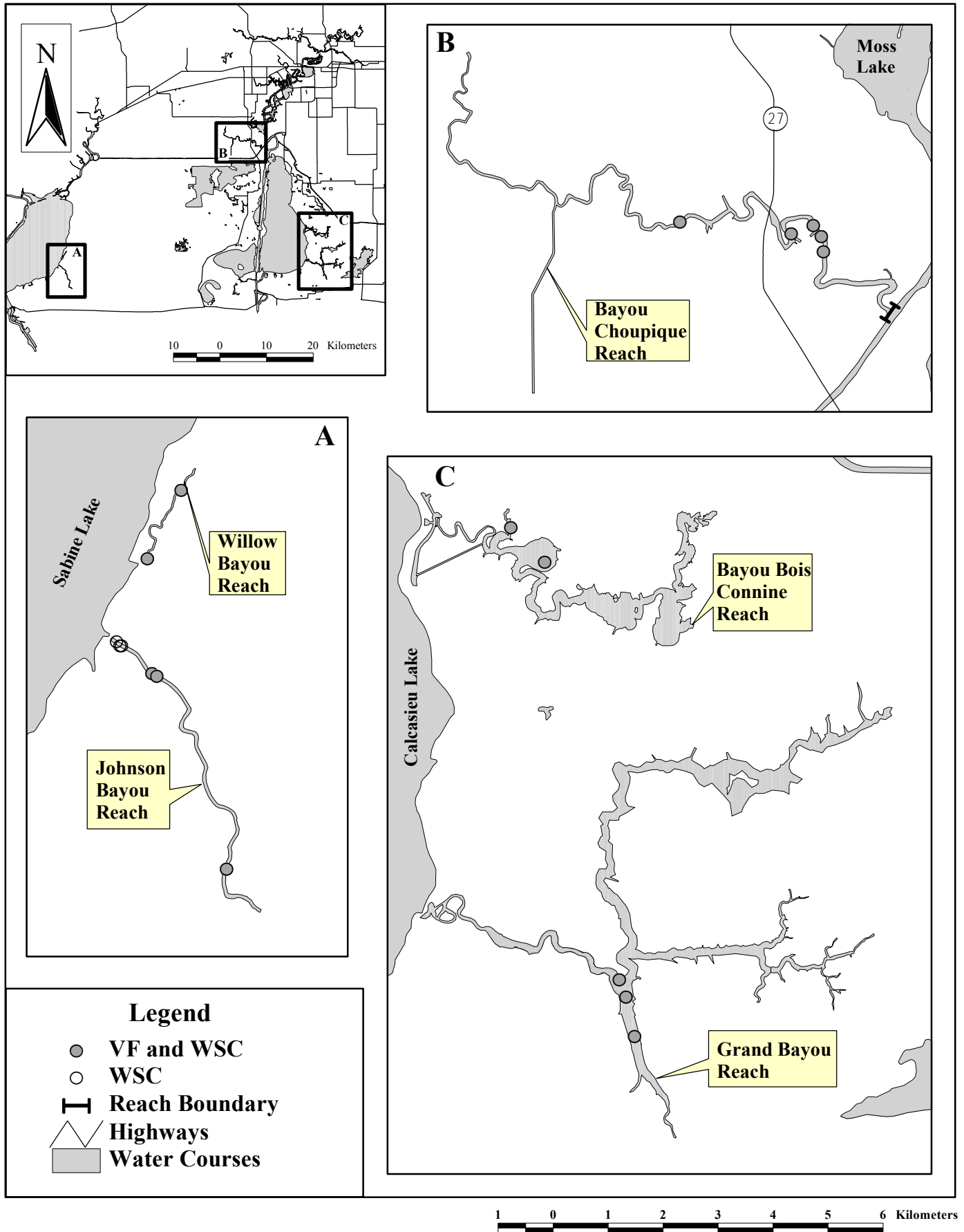


Figure C-6a. Map of the Upper Calcasieu River AOC, showing the reach boundaries and locations of surficial sediment samples that pose low or high risk to microorganisms, based on comparisons of whole-sediment chemistry data to the selected benchmarks (i.e., one or more exceedances of the Microtox™ AETs).

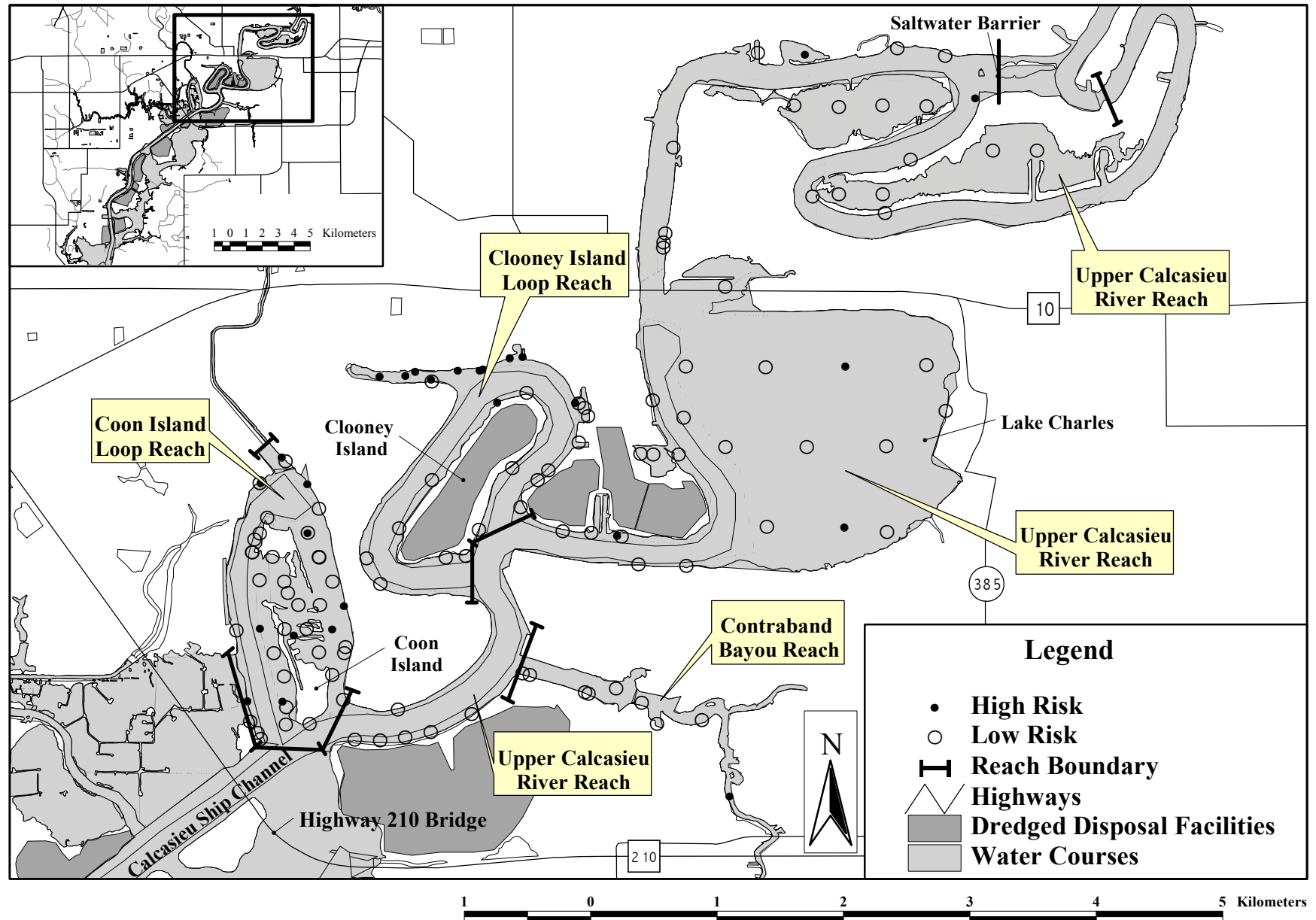


Figure C-6b. Map of the Upper Calcasieu River AOC, showing the reach boundaries and locations of deeper sediment samples that pose low or high risk to microorganisms, based on comparisons of whole-sediment chemistry data to the selected benchmarks (i.e., one or more exceedances of the Microtox™ AETs).

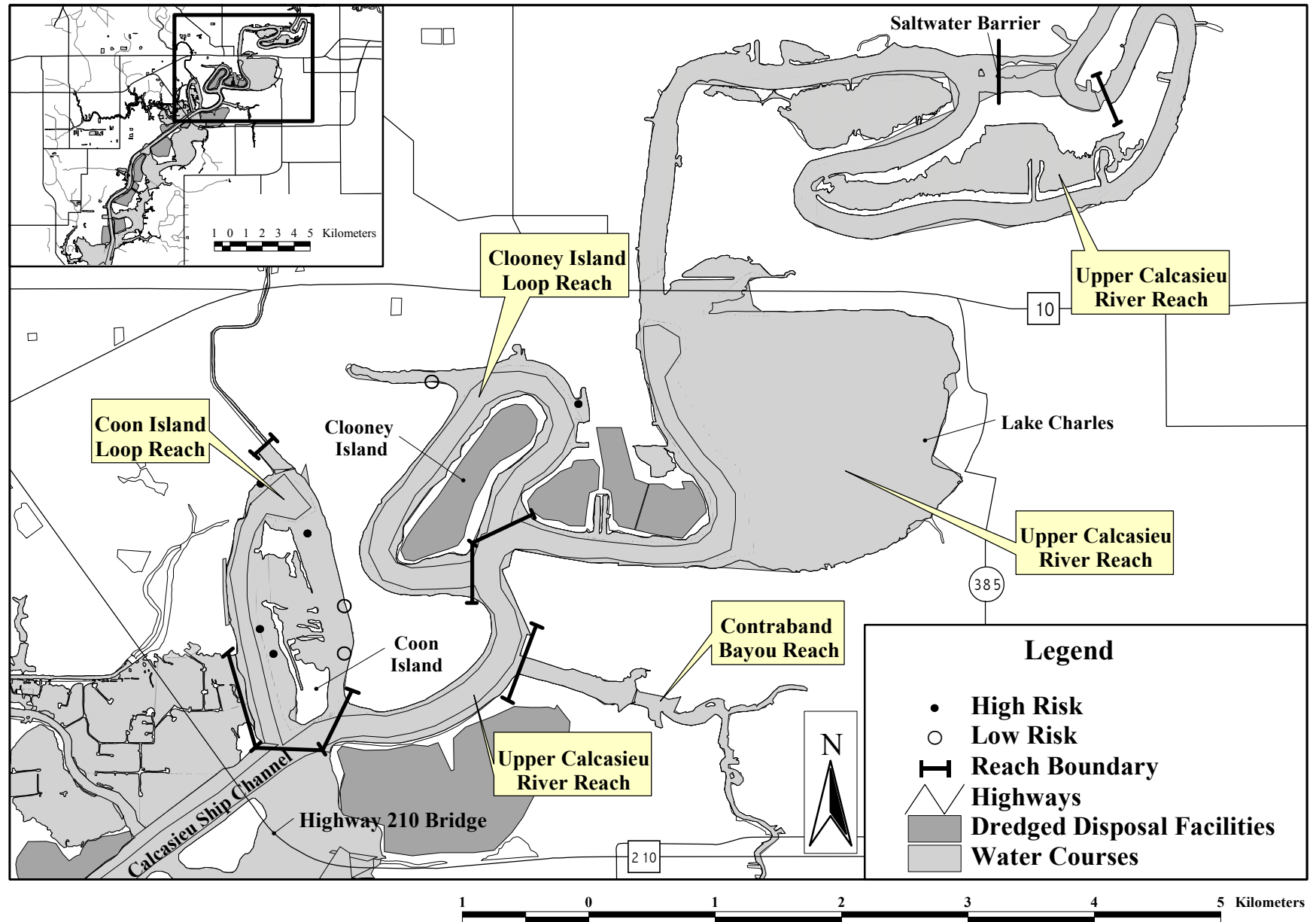


Figure C-7. Map of the Upper Calcasieu River AOC, showing the reach boundaries and locations of toxic and not toxic samples, based on the results of solid phase tests with the bacterium, *Vibrio fisheri* (based on the reference envelope approach).

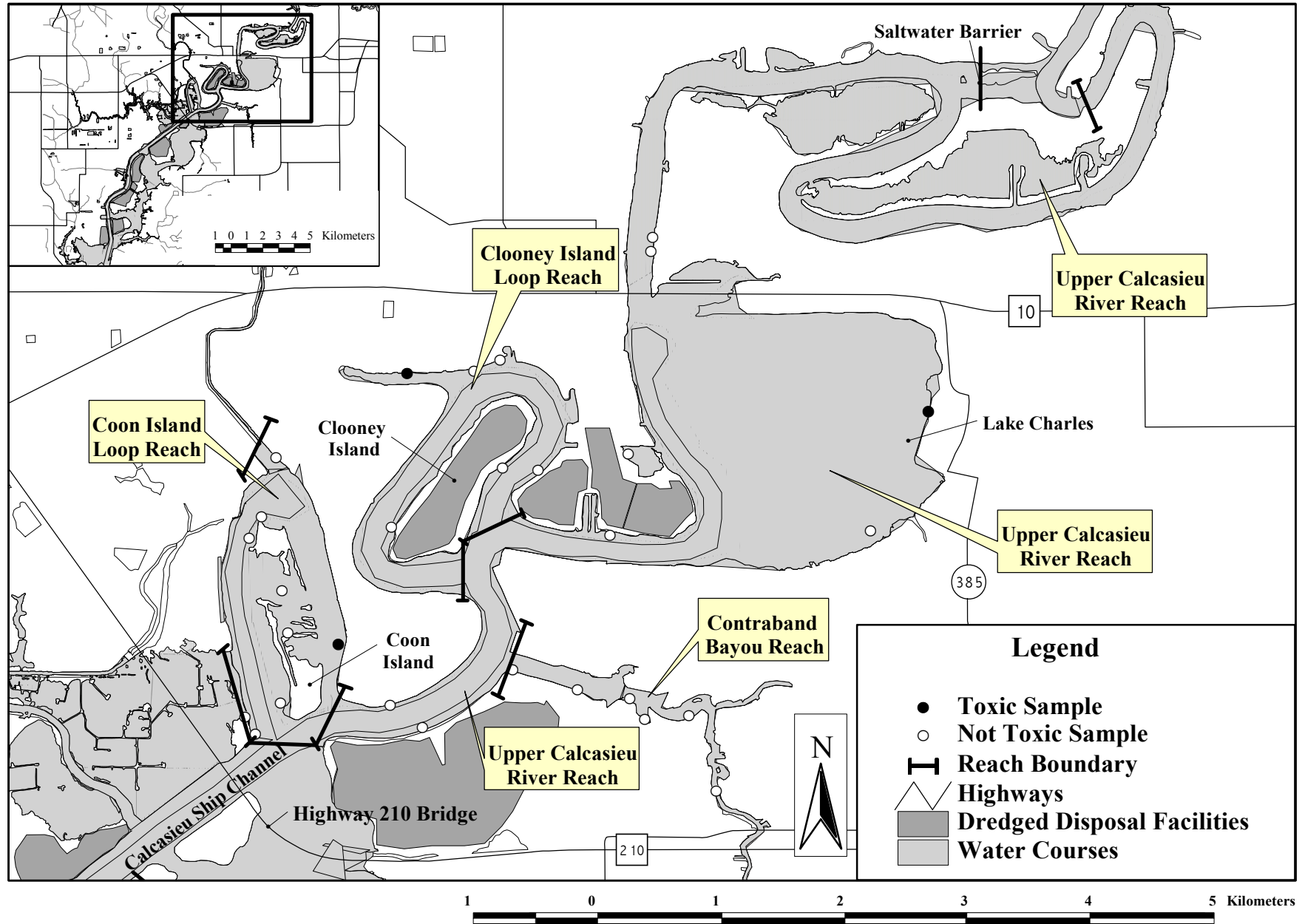


Figure C-8. Cumulative frequency distribution of 1,1'-biphenyl in whole-sediment samples evaluated using the results of the 25-m solid phase tests with the bacterium, *Vibrio fischeri* (endpoint: EC₅₀-bioluminescence). The dashed line represents the selected benchmark for 1,1'-biphenyl.

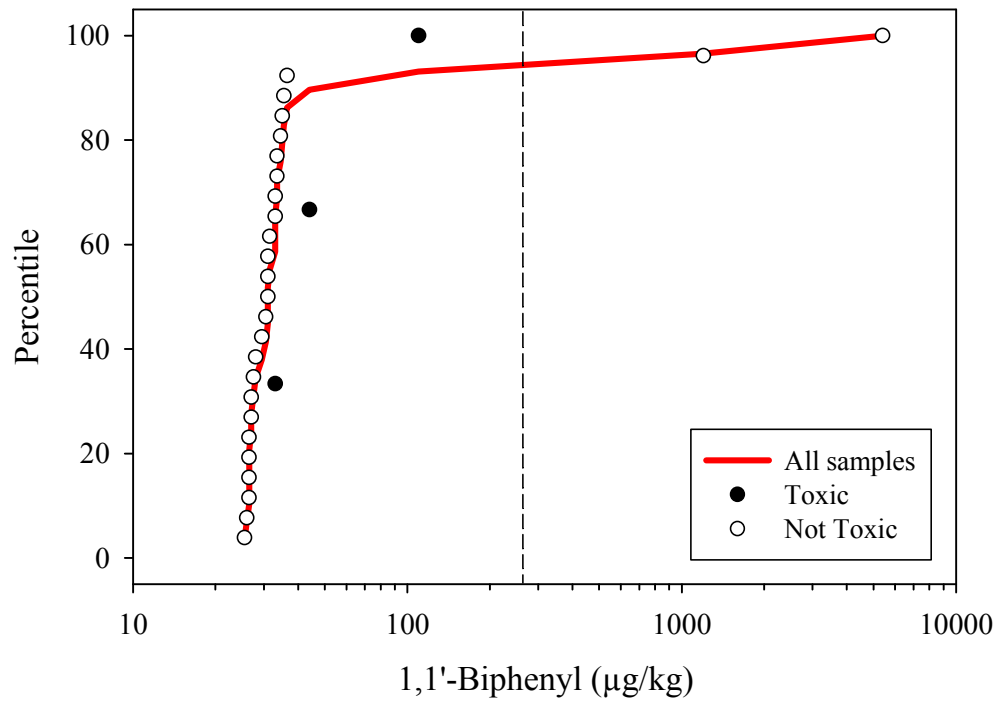


Figure C-9. Cumulative frequency distribution of 2-methylnaphthalene in whole-sediment samples evaluated using the results of the 25-m solid phase tests with the bacterium, *Vibrio fischeri* (endpoint: EC₅₀-bioluminescence). The dashed line represents the selected benchmark for 2-methylnaphthalene.

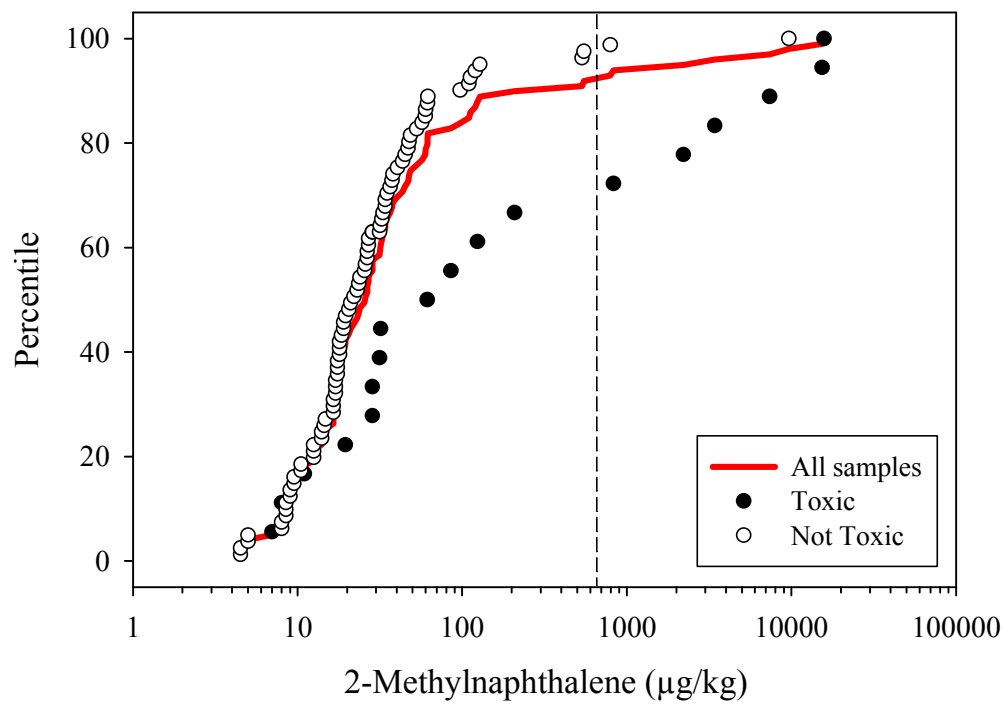


Figure C-10. Cumulative frequency distribution of acenaphthene in whole-sediment samples evaluated using the results of the 25-m solid phase tests with the bacterium, *Vibrio fischeri* (endpoint: EC₅₀-bioluminescence). The dashed line represents the selected benchmark for acenaphthene.

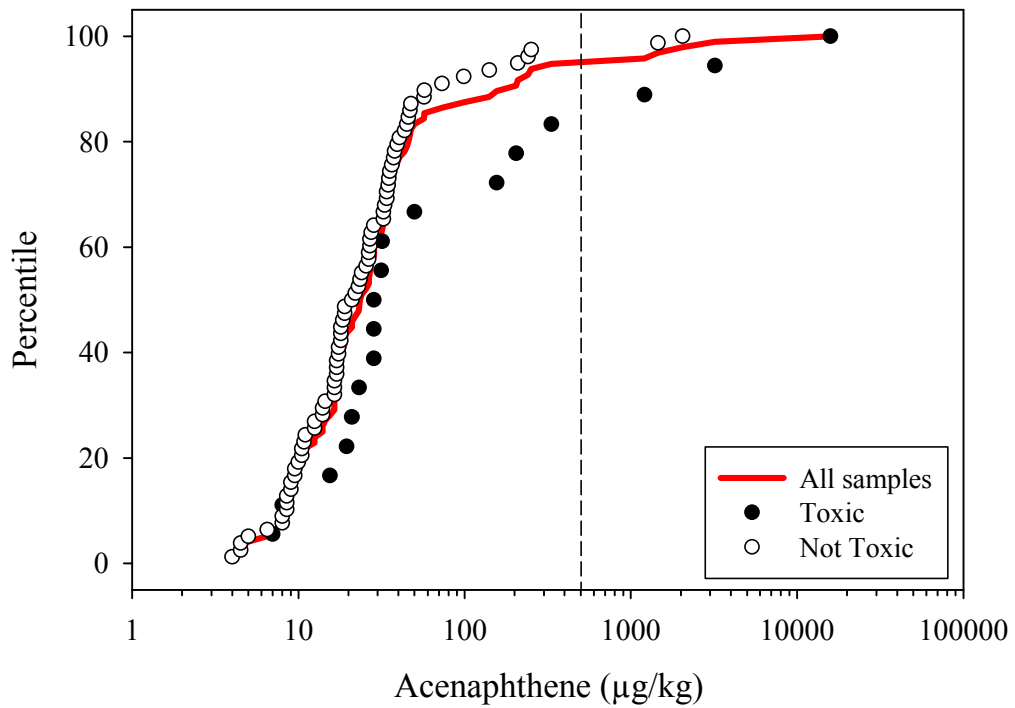


Figure C-11. Cumulative frequency distribution of acenaphthylene in whole-sediment samples evaluated using the results of the 25-m solid phase tests with the bacterium, *Vibrio fischeri* (endpoint: EC₅₀-bioluminescence). The dashed line represents the selected benchmark for acenaphthylene.

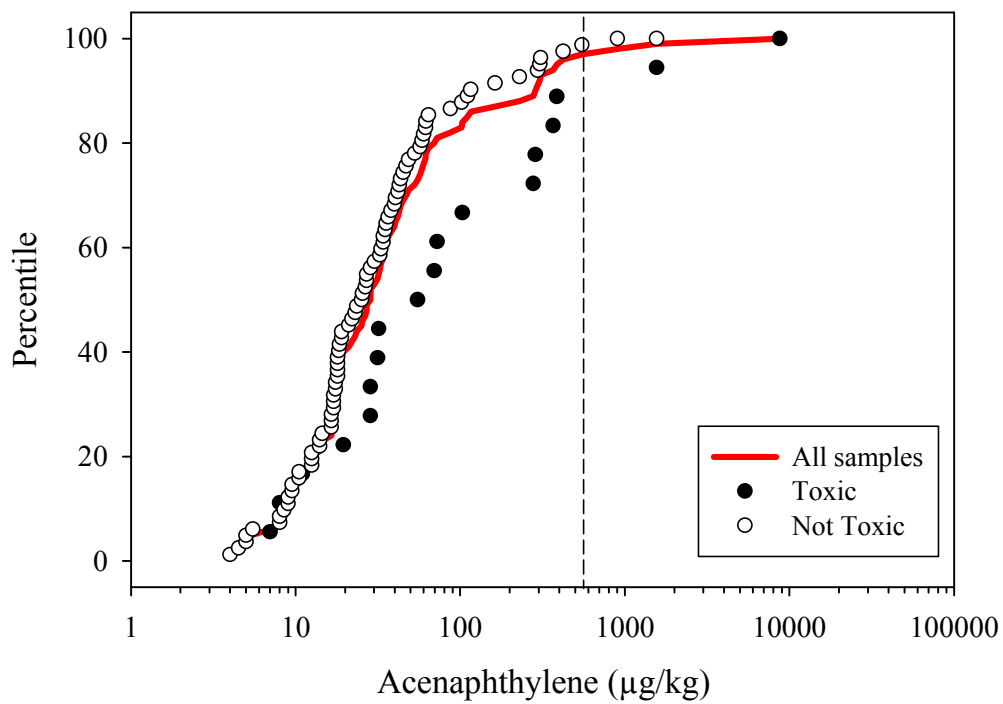


Figure C-12. Cumulative frequency distribution of anthracene in whole-sediment samples evaluated using the results of the 25-m solid phase tests with the bacterium, *Vibrio fischeri* (endpoint: EC₅₀-bioluminescence). The dashed line represents the selected benchmark for anthracene.

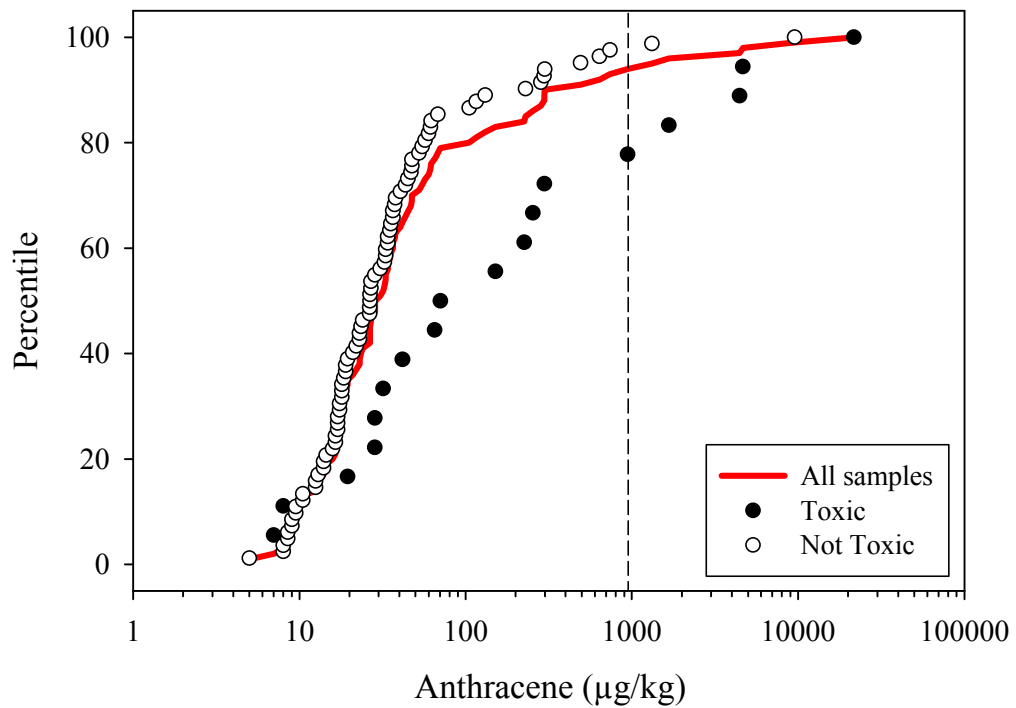


Figure C-13. Cumulative frequency distribution of fluorene in whole-sediment samples evaluated using the results of the 25-m solid phase tests with the bacterium, *Vibrio fischeri* (endpoint: EC₅₀-bioluminescence). The dashed line represents the selected benchmark for fluorene.

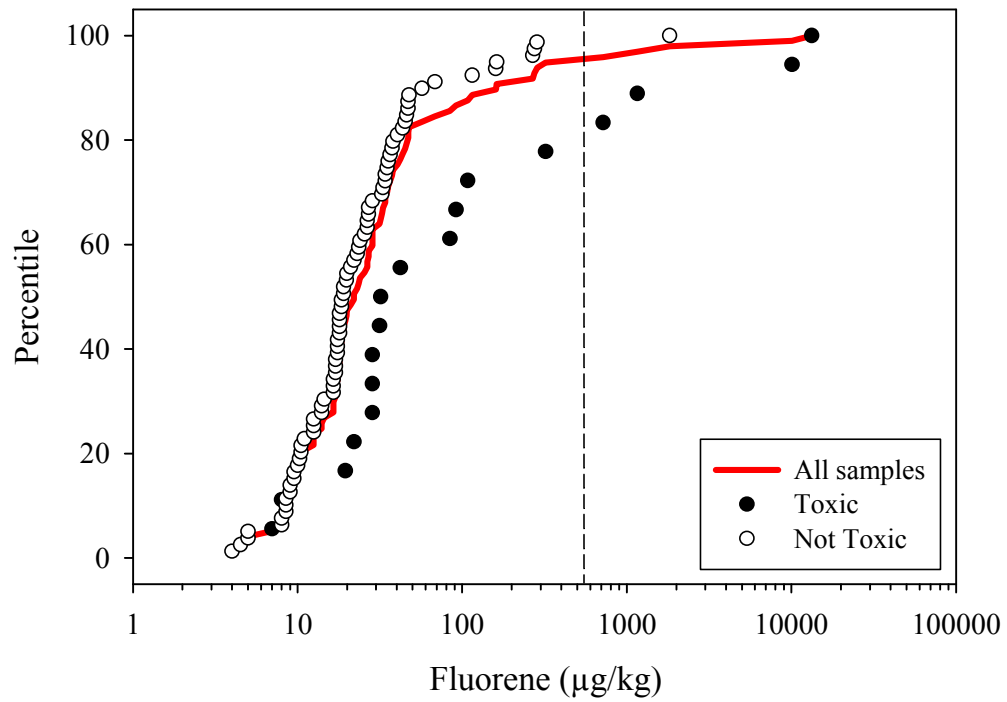


Figure C-14. Cumulative frequency distribution of naphthalene in whole-sediment samples evaluated using the results of the 25-m solid phase tests with the bacterium, *Vibrio fischeri* (endpoint: EC₅₀-bioluminescence). The dashed line represents the selected benchmark for naphthalene.

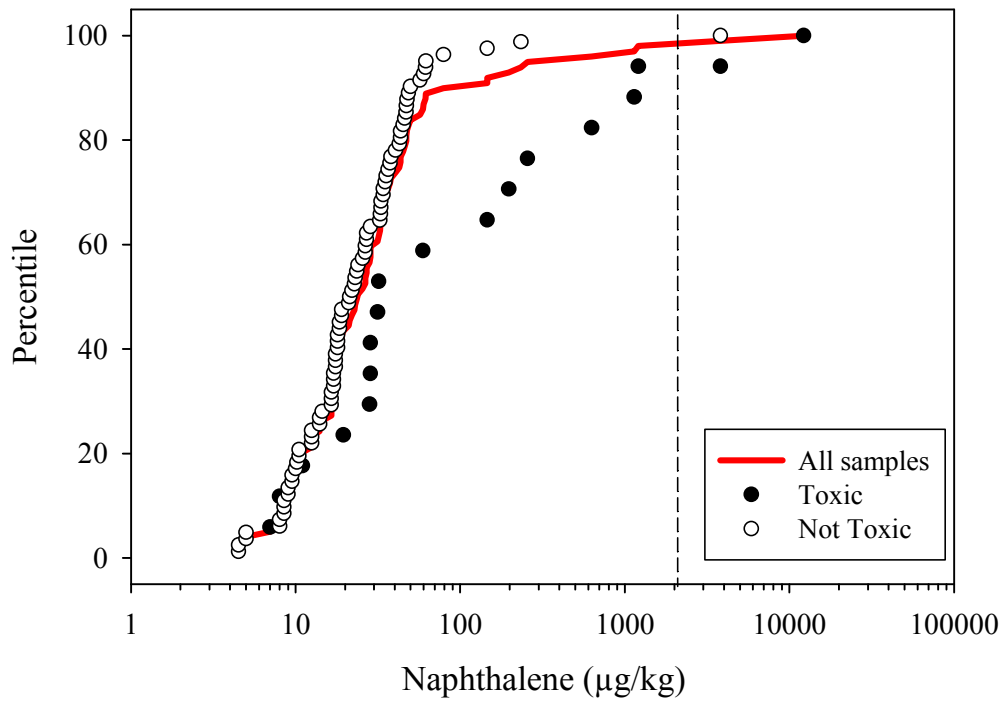


Figure C-15. Cumulative frequency distribution of phenanthrene in whole-sediment samples evaluated using the results of the 25-m solid phase tests with the bacterium, *Vibrio fischeri* (endpoint: EC₅₀-bioluminescence). The dashed line represents the selected benchmark for phenanthrene.

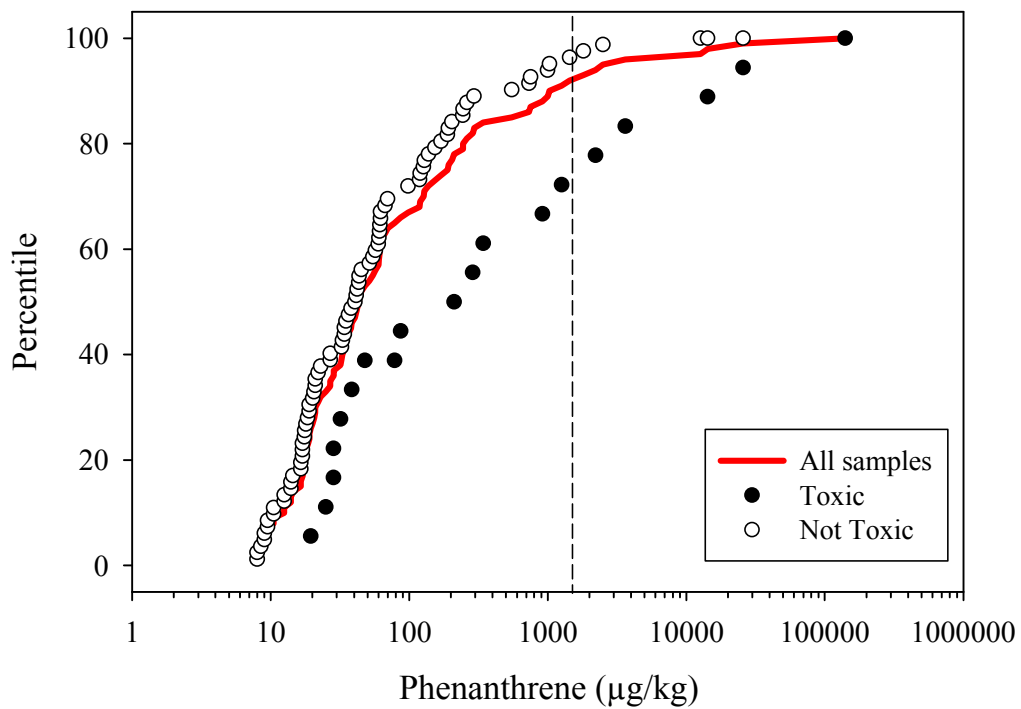


Figure C-16. Cumulative frequency distribution of total low molecular weight PAHs in whole-sediment samples evaluated using the results of the 25-m solid phase tests with the bacterium, *Vibrio fischeri* (endpoint: EC₅₀ bioluminescence). The dashed line represents the selected benchmark for total low molecular weigh PAHs.

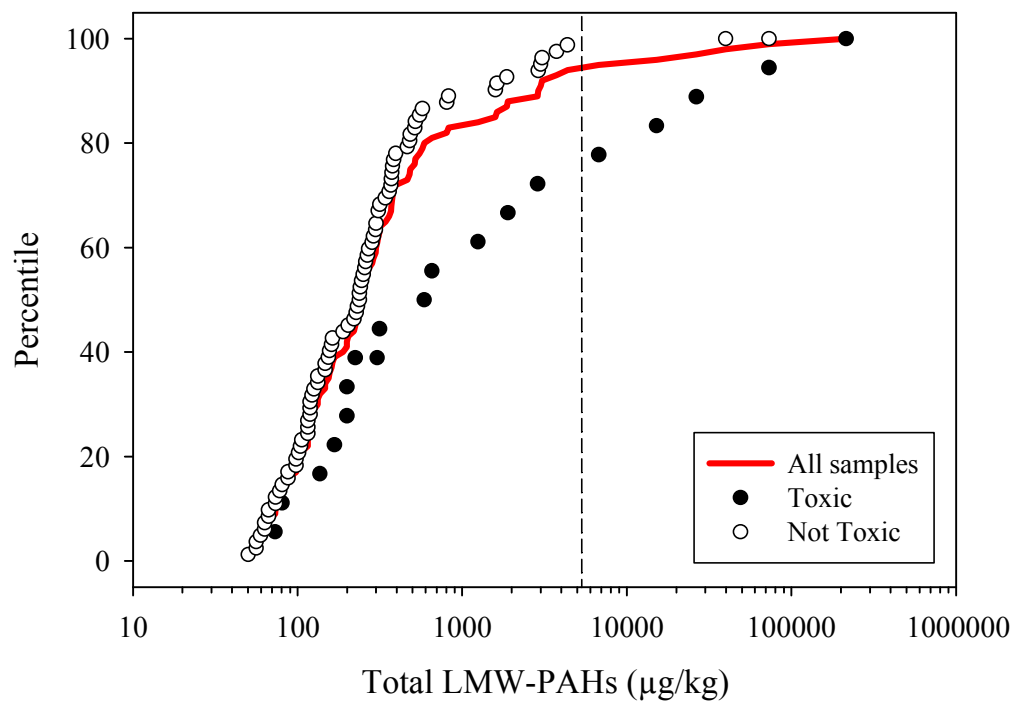


Figure C-17. Cumulative frequency distribution of benz(a)anthracene in whole-sediment samples evaluated using the results of the 25-m solid phase tests with the bacterium, *Vibrio fischeri* (endpoint: EC₅₀-bioluminescence). The dashed line represents the selected benchmark for benz(a)anthracene.

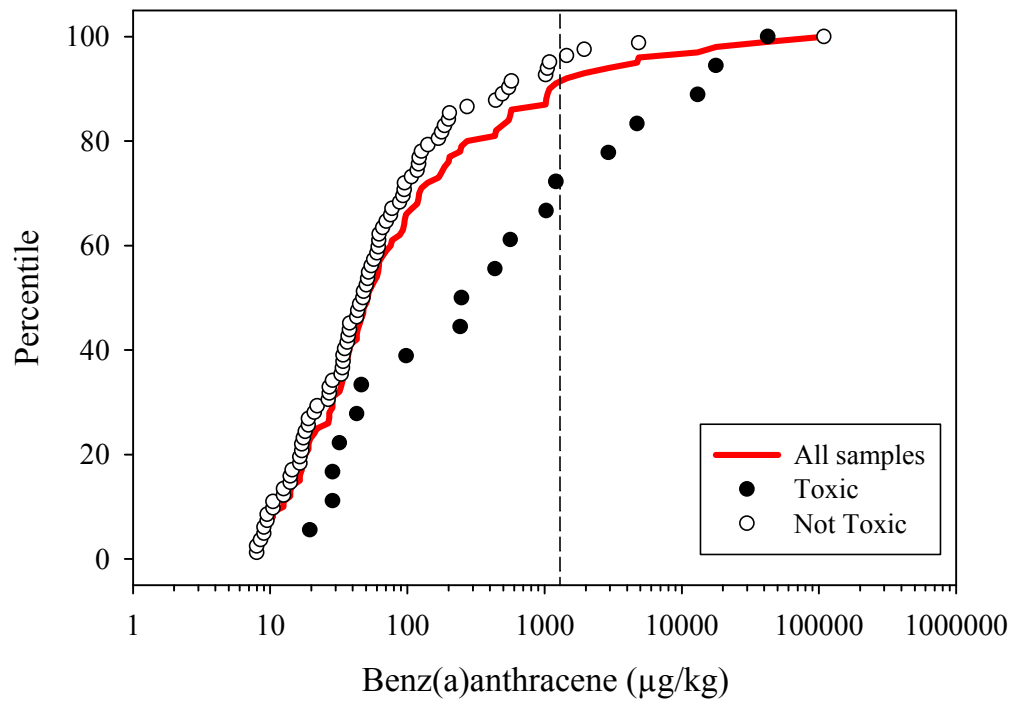


Figure C-18. Cumulative frequency distribution of benzo(a)pyrene in whole-sediment samples evaluated using the results of the 25-m solid phase tests with the bacterium, *Vibrio fischeri* (endpoint: EC₅₀-bioluminescence). The dashed line represents the selected benchmark for benzo(a)pyrene.

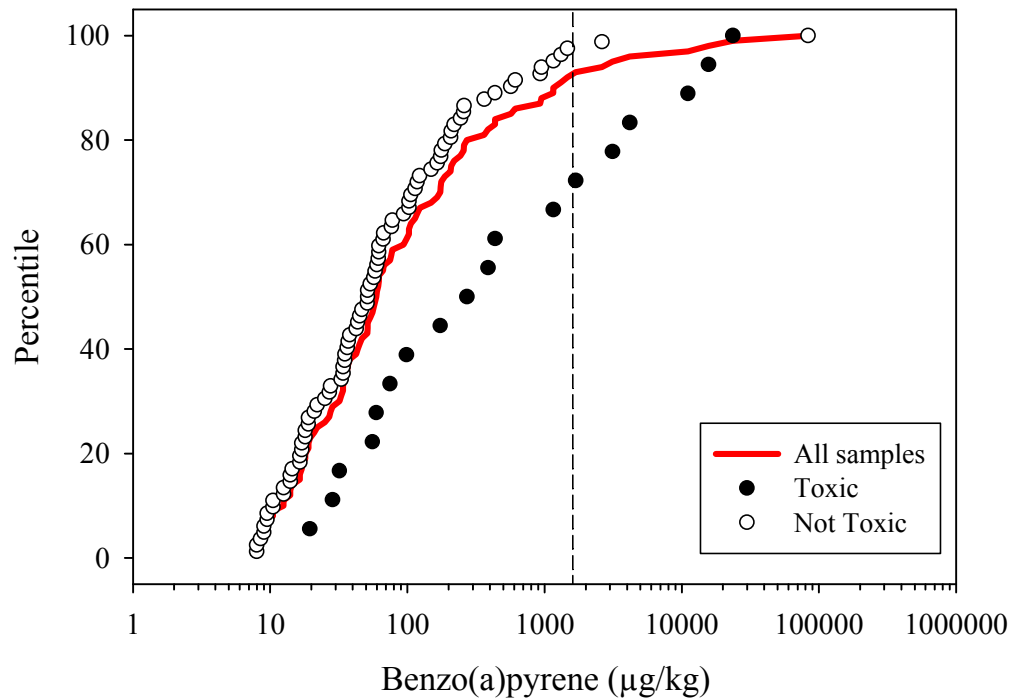


Figure C-19. Cumulative frequency distribution of benzo(b)fluoranthene in whole-sediment samples evaluated using the results of the 25-m solid phase tests with the bacterium, *Vibrio fischeri* (endpoint: EC₅₀-bioluminescence). The dashed line represents the selected benchmark for benzo(b)fluoranthene.

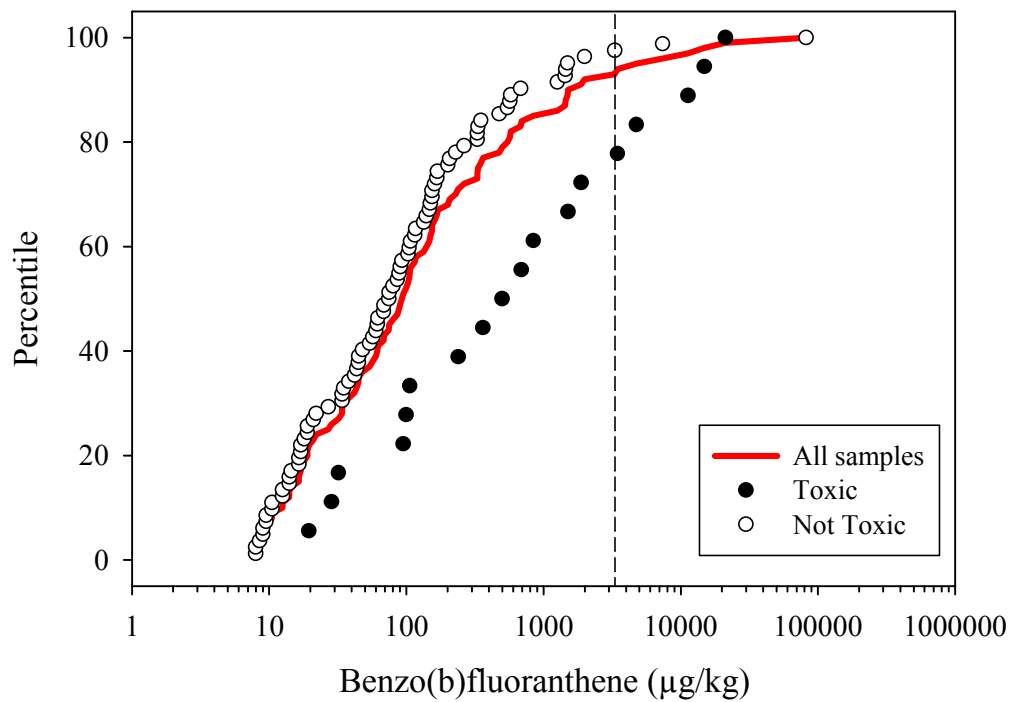


Figure C-20. Cumulative frequency distribution of benzo(g,h,i)perylene in whole-sediment samples evaluated using the results of the 25-m solid phase tests with the bacterium, *Vibrio fischeri* (endpoint: EC₅₀-bioluminescence). The dashed line represents the selected benchmark for benzo(g,h,i)perylene.

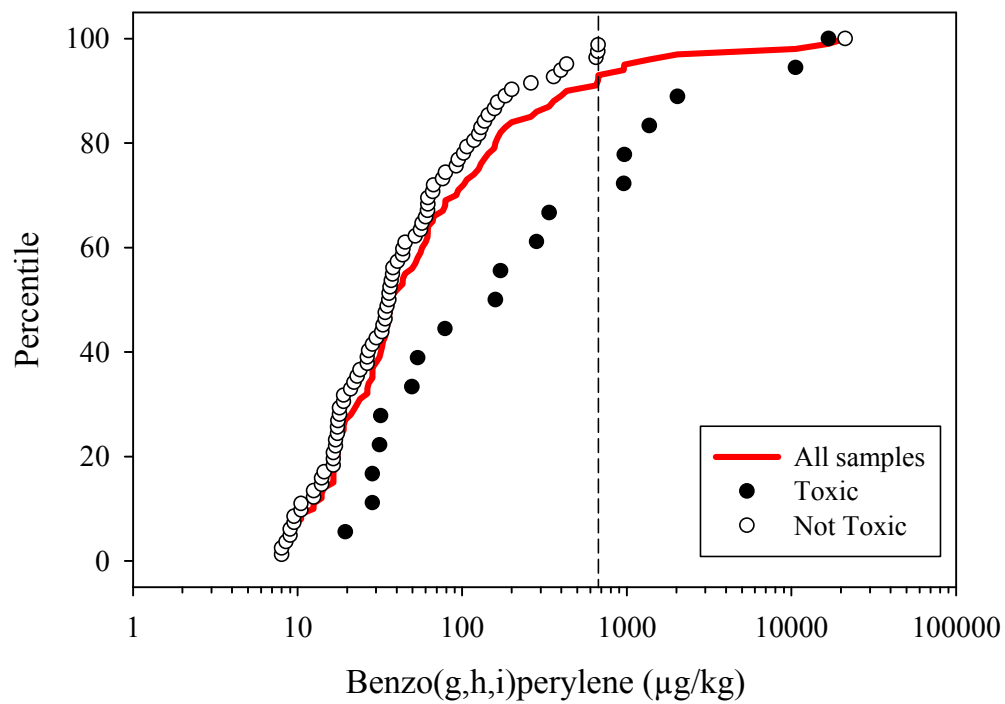


Figure C-21. Cumulative frequency distribution of benzo(k)fluoranthene in whole-sediment samples evaluated using the results of the 25-m solid phase tests with the bacterium, *Vibrio fischeri* (endpoint: EC₅₀-bioluminescence). The dashed line represents the selected benchmark for benzo(k)fluoranthene.

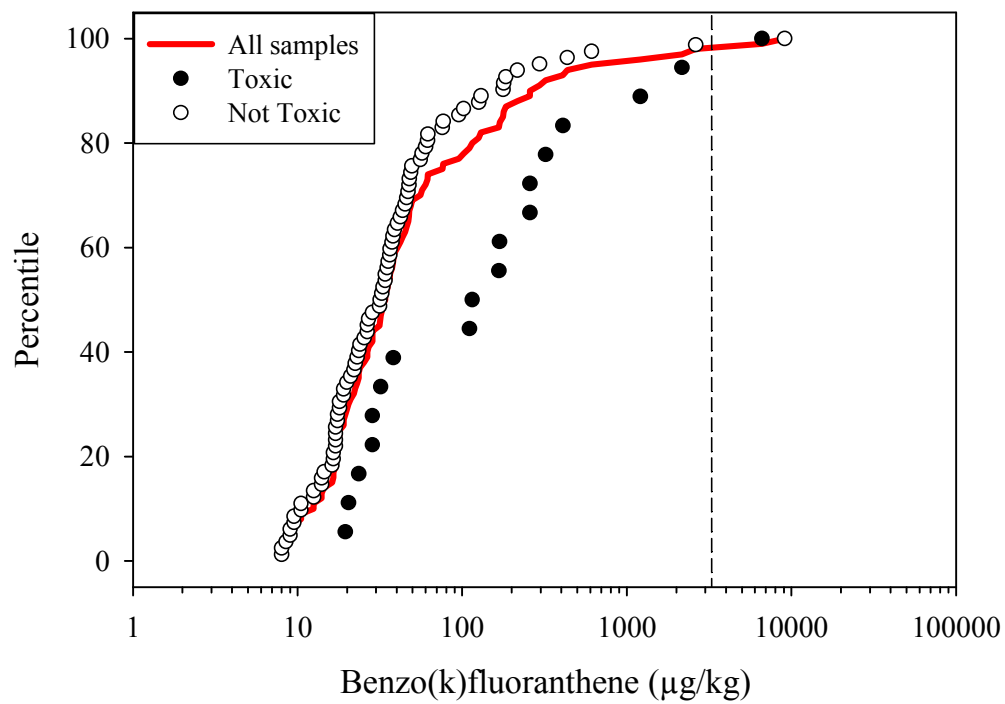


Figure C-22. Cumulative frequency distribution of chrysene in whole-sediment samples evaluated using the results of the 25-m solid phase tests with the bacterium, *Vibrio fischeri* (endpoint: EC₅₀-bioluminescence). The dashed line represents the selected benchmark for chrysene.

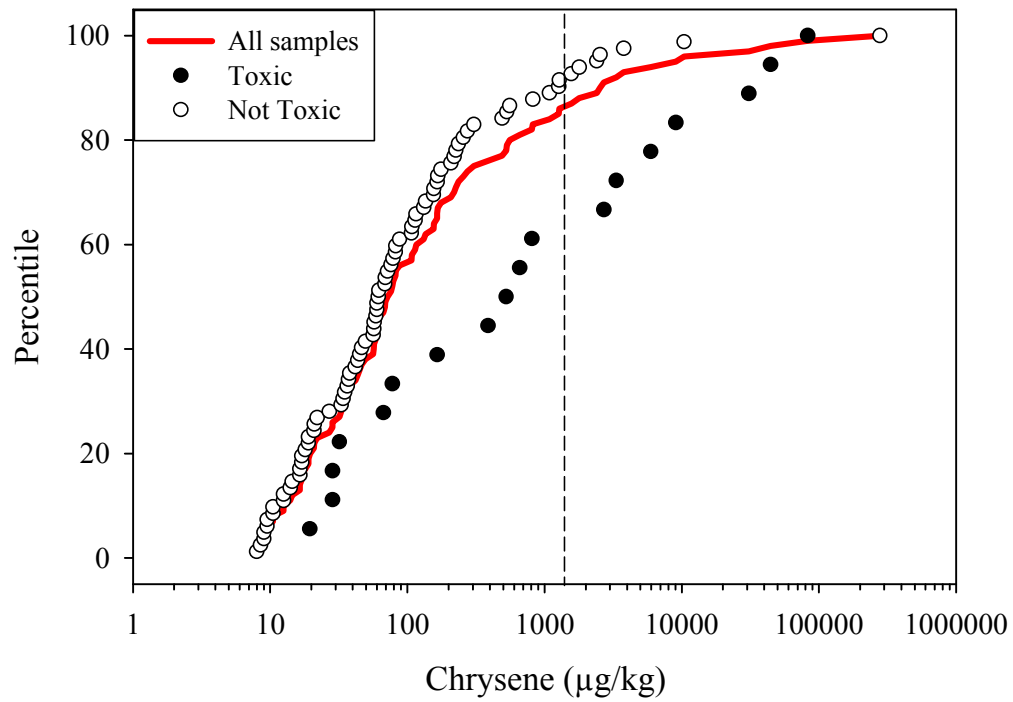


Figure C-23. Cumulative frequency distribution of dibenz(a,h)anthracene in whole-sediment samples evaluated using the results of the 25-m solid phase tests with the bacterium, *Vibrio fischeri* (endpoint: EC₅₀-bioluminescence). The dashed line represents the selected benchmark for dibenz(a,h)anthracene.

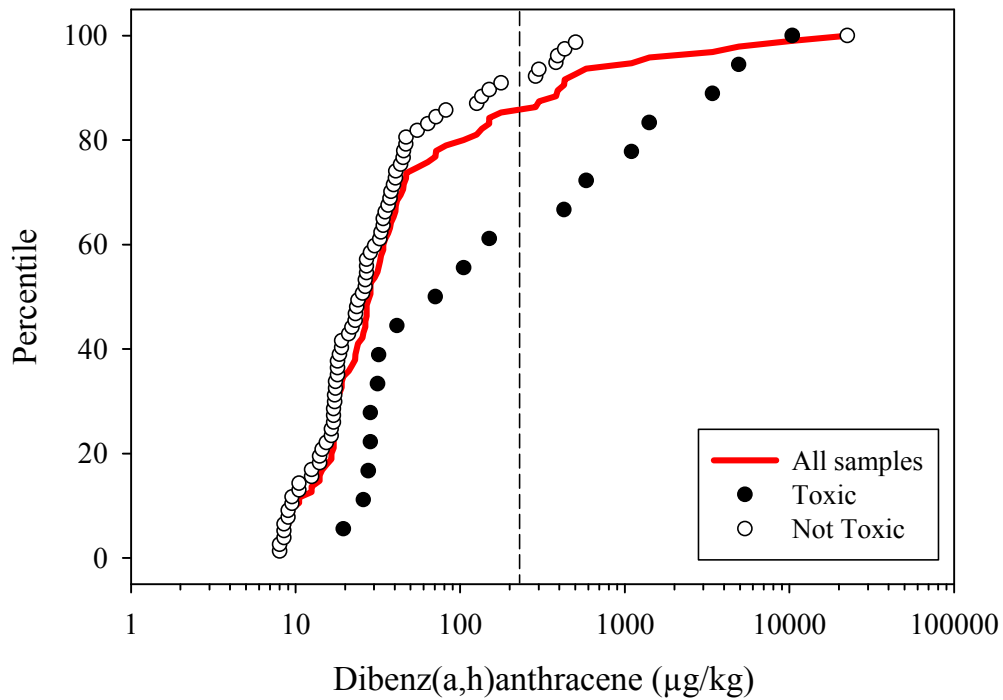


Figure C-24. Cumulative frequency distribution of indeno(1,2,3-cd)pyrene in whole-sediment samples evaluated using the results of the 25-m solid phase tests with the bacterium, *Vibrio fischeri* (endpoint: EC₅₀-bioluminescence). The dashed line represents the selected benchmark for indeno(1,2,3-cd)pyrene.

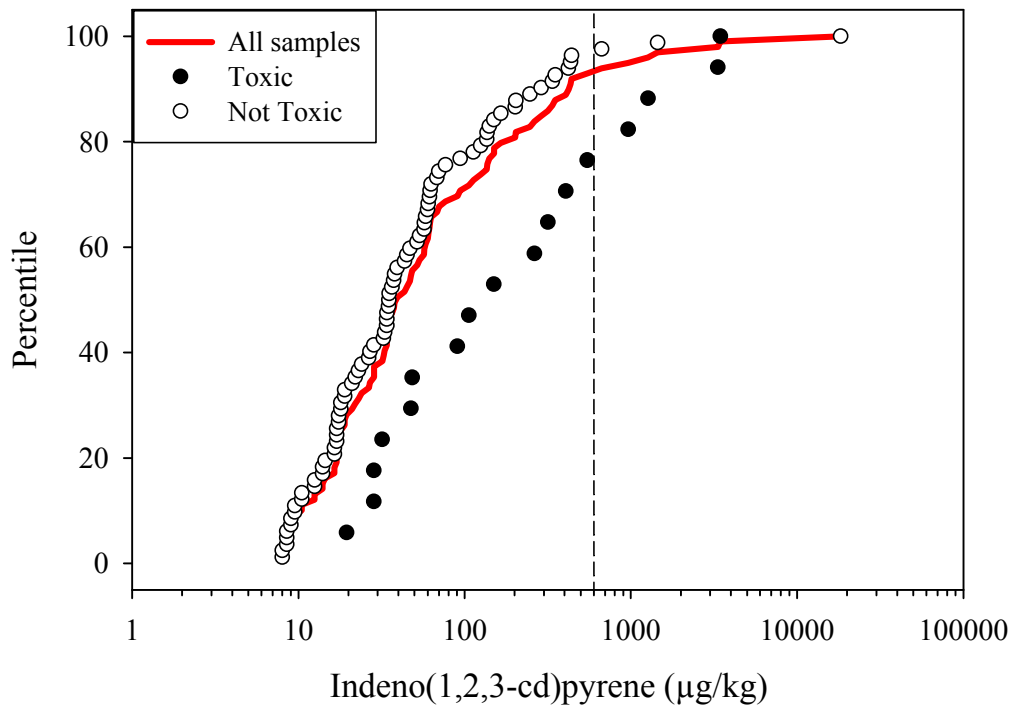


Figure C-25. Cumulative frequency distribution of fluoranthene in whole-sediment samples evaluated using the results of the 25-m solid phase tests with the bacterium, *Vibrio fischeri* (endpoint: EC₅₀-bioluminescence). The dashed line represents the selected benchmark for fluoranthene.

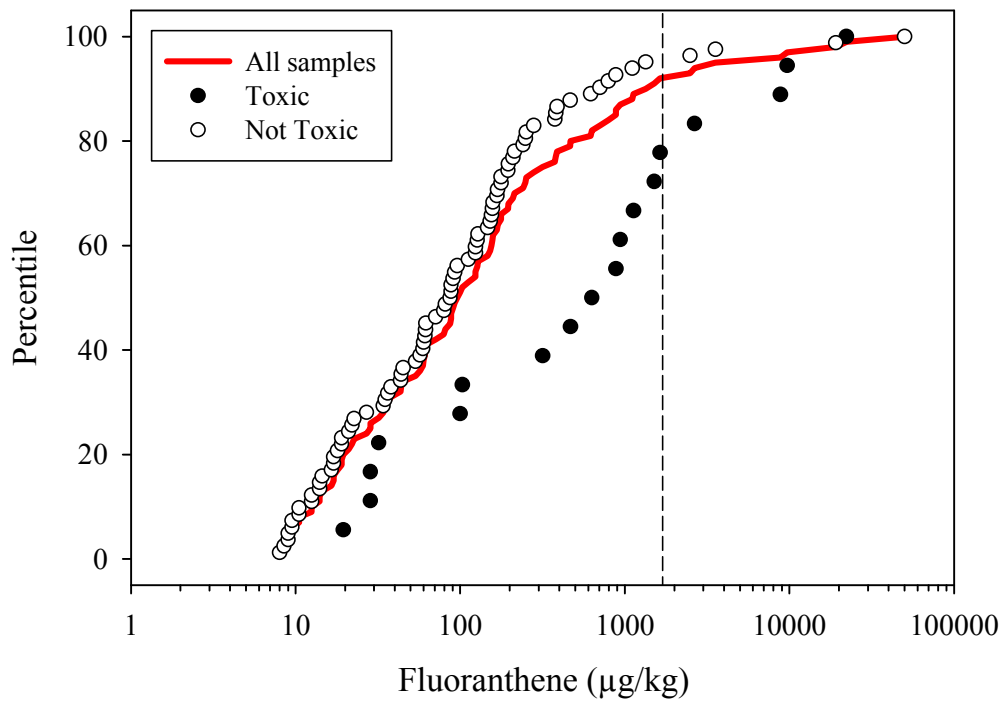


Figure C-26. Cumulative frequency distribution of pyrene in whole-sediment samples evaluated using the results of the 25-m solid phase tests with the bacterium, *Vibrio fischeri* (endpoint: EC₅₀-bioluminescence). The dashed line represents the selected benchmark for pyrene.

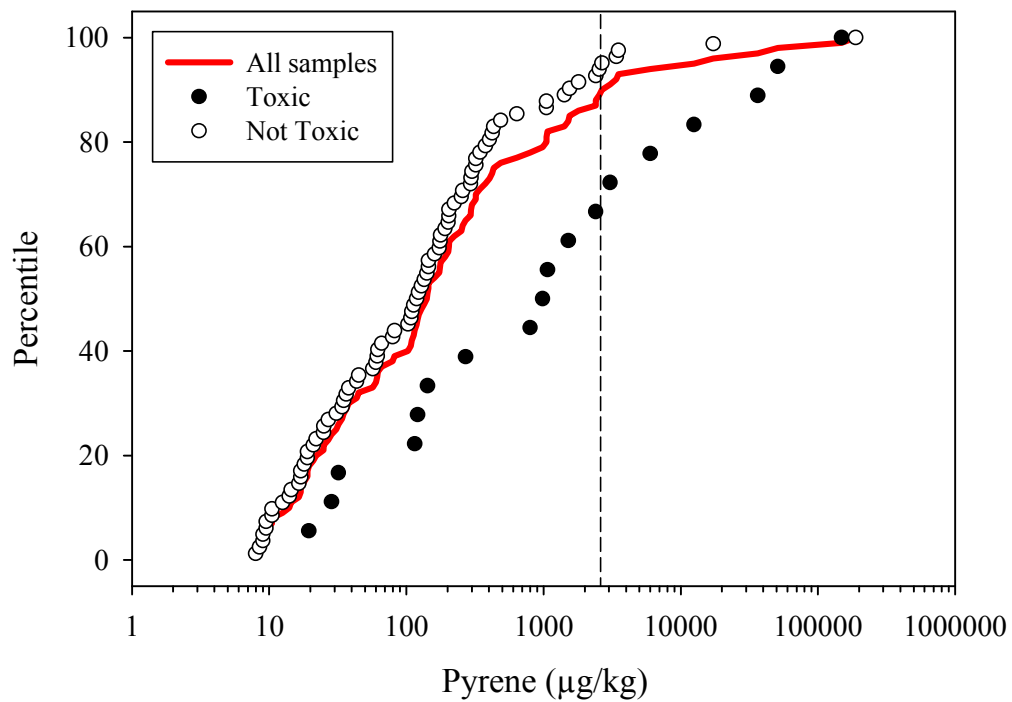


Figure C-27. Cumulative frequency distribution of total high molecular weight PAHs in whole-sediment samples evaluated using the results of the 25-m solid phase tests with the bacterium, *Vibrio fischeri* (endpoint: EC₅₀-bioluminescence). The dashed line represents the selected benchmark for total high molecular weight PAHs.

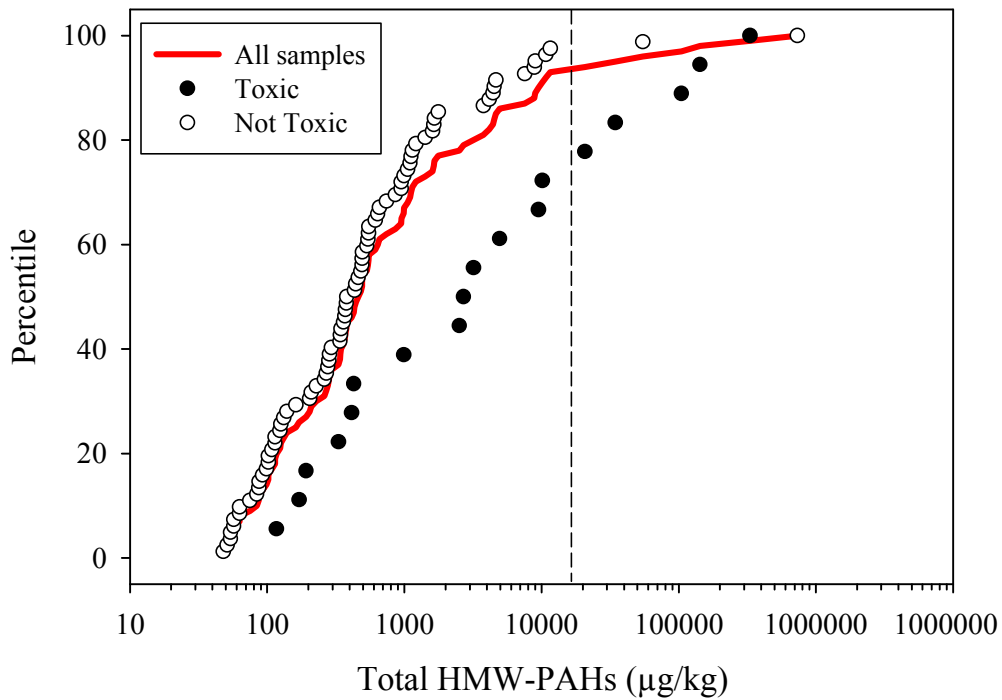


Figure C-28. Cumulative frequency distribution of total PAHs in whole-sediment samples evaluated using the results of the 25-m solid phase tests with the bacterium, *Vibrio fischeri* (endpoint: EC₅₀-bioluminescence). The dashed line represents the selected benchmark for total PAHs.

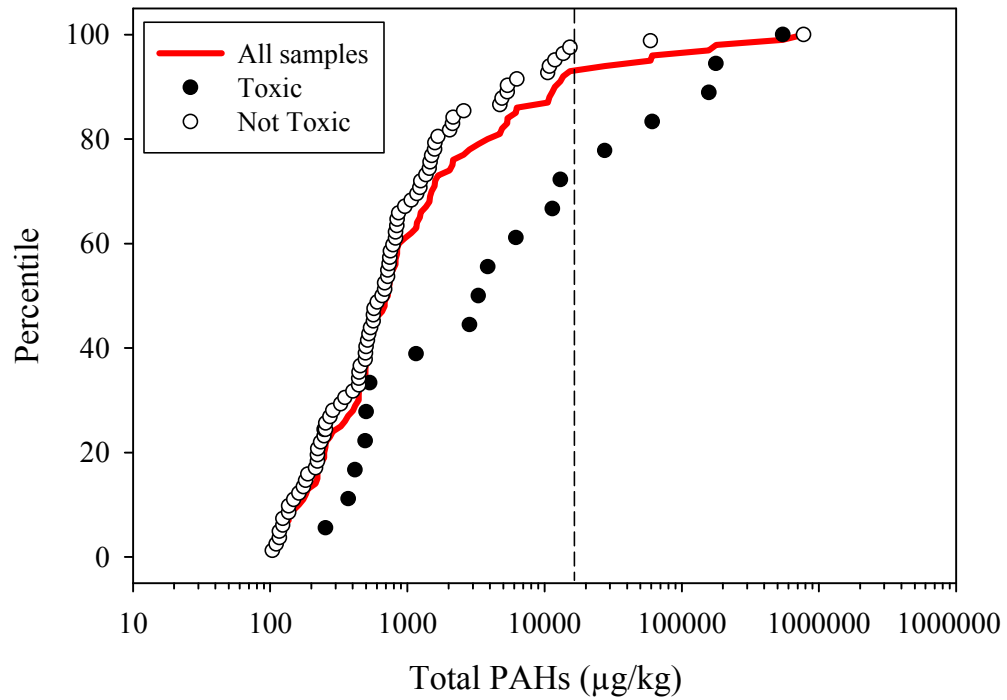


Figure C-29. Cumulative frequency distribution of total PCBs in whole-sediment samples evaluated using the results of the 25-m solid phase tests with the bacterium, *Vibrio fischeri* (endpoint: EC₅₀-bioluminescence). The dashed line represents the selected benchmark for total PCBs.

